International Journal of Advanced Research in Engineering and Applied Sciences

ISSN: 2278-6252

A NUMERICAL STUDY ON DEVELOPED LAMINAR MIXED CONVECTION IN VERTICAL CHANNEL WITH DISSIPATION

T. Gopal Reddy*

M. Rama Chandra Reddy**

B. Rama Bhupal Reddy***

Abstract: *A numerical study on developed laminar mixed convection in vertical channels is considered. The flow problem is described by means of partial differential equations and the solutions are obtained by an implicit finite difference technique coupled with a marching procedure. The velocity, the temperature and the pressure profiles are obtained and their behaviour is discussed computationally for different values of governing parameters like buoyancy parameter Gr/Re, the wall temperature difference ratio rT, the Eckert Number Ek and Prandle number Pr. The analysis of the obtained results showed that the flow is significantly influenced by these governing parameters.*

Keywords: *Mixed convection, Vertical channel, Dissipation*

*Jr. Lecturer in Mathematics, Government Junior College, Kurnool, A.P., India

**Reader in Mathematics, S.K.S.C. Degree College, Proddatur, A.P., India

***Associate Professor in Mathematics, K.S.R.M. College of Engineering, Kadapa, A.P., India

1. INTRODUCTION

Understanding the flow development is essential in the analysis of the flow of heat as well as the development of temperature and other heat transfer parameters. The research related to flow and heat transfer through parallel plate channels has been well cited by Inagaki and Komori [10]. The literature pertinent to mixed convection in vertical channels between vertical parallel plates is reviewed hereunder and is divided according to the flow status (i.e., fully developed or developing). For laminar flow, in the fully developed region, i.e., in the region far from the channel entrance, the fluid velocity does not undergo appreciable changes in the stream-wise direction. Under these conditions, mixed convection between vertical parallel plates has been of interest in research for many years. Early work includes studies by Cebeci et al. [6] and by Aung and Worku [2]. The work by these investigators has shown that mixed convection between parallel plates exhibits both similarities and contrasts with flow in a vertical tube. Reddy [12] studied on developed laminar mixed convection in vertical channels. With the technological demand on heat transfer enhancement, most markedly related to compact heat exchangers, solar energy collection, as in the conventional flat plate collector and cooling of electronic equipment analysis, the parallel-plate channel geometry gained further attention from thermal engineering researchers.

Using dimensionless parameters, Aung and Worku [2] solved the problem of mixed convection between parallel plates and obtained closed form analytical solution. From the closed form solution for U, the criterion for the existence of reversed flow has been deduced under thermal boundary conditions of uniform heating on one wall while the other wall was thermally insulated. The relations between the Nusselt number and the Rayleigh number, and between the friction factor times the Reynolds number and the Rayleigh number were presented. For assisted flow, the Nusselt number increases with the Rayleigh number, while the opposite is true for opposed flow. The behaviour of the product of friction factor and Reynolds number is similar to that of the Nusselt number. In general, these behaviours are similar to those for laminar flow in a uniformly heated vertical tube. Recently, Boulama and Galanis [5] presented exact solutions for fully developed, steady state laminar mixed convection between parallel plates with heat and mass transfer under the thermal boundary conditions of (uniform wall temperature) UWT and (uniform heat

flux) UHF. The results revealed that buoyancy effects significantly improve heat and momentum transfer rates near heated walls of the channel. They [5] also analyzed the conditions for flow reversal.

To analyze the behaviour of the flow with opposing buoyancy forces, Hamadah and Wirtz [7] studied the laminar mixed convection under three different thermal boundary conditions (i.e., both walls isothermal, both walls at constant heat flux and one wall at constant heat flux and other is maintained at constant temperature). They obtained closed form solutions to the fully developed governing equations and found that the heat transfer rates are dependent on Gr/Re and the ratio of wall thermal boundary. In their analysis, they obtained values of Gr/Re beyond which flow reversal takes place. The vertical parallel plate configuration is applicable in the design of cooling systems for electronic equipment and of finned cold plates in general. In such systems, where the height of the channel is small, developing flow mode should be applicable.

An analysis of the mixed convection in a channel provides information on the flow structure in the developing region and reveals the different length scales accompanying the different convective mechanisms operative in the developing flow region. Yao [15] studied mixed convection in a channel with symmetric uniform temperature and symmetric uniform flux heating. He presented no quantitative information; he conjectured that fully developed flow might consist of periodic reversed flow. Quantitative information on the temperature and velocity fields has been provided in a numerical study reported by Aung and Worku [1]. These authors noted that buoyancy effects dramatically increase the hydrodynamic development distance. With asymmetric heating, the bulk temperature is a function of Gr/Re and r_T, and decreases as r_T is reduced. Buoyancy effects are noticeable through a large segment of the channel, but not near the channel entrance or far downstream from it.

Wirtz and Mckinley [14] conducted laboratory experiments on downward mixed convection between parallel plates where one plate heated the fluid (i.e., buoyancy-opposed flow situation). A laminar developing flow was observed in the absence of heating. The initial application of a plate heat flux resulted in a shifting of the mass flux profile away from the heated wall, a reduction in mass flow rate between the plates, and a corresponding decrease in plate heat transfer coefficient. A large application of plate heat flux resulted in a continuous decrease in mass flow rate with an increase in plate heat transfer coefficient.

Turbulence intensity measurements suggested that the heating destabilizes the flow adjacent to the wall, giving rise to an increase in convective transport, which ultimately offsets the effect of the reduction in flow rate. These results suggest that a computation model of mixed convection applied to this flow geometry will require a turbulence model which includes buoyancy force effects, even at flow rates normally associated with laminar convection. Ingham et al. [11] presented a numerical investigation for the steady laminar combined convection flows in vertical parallel plate ducts with asymmetric constant wall temperature boundary conditions. Reversed flow has been recorded in the vicinity of the cold wall for some combinations of the ratio (Gr/Re) and the difference in the temperature between the walls. It was concluded that for a fixed value of r_T (value of the dimensionless temperature at the wall) heat transfer is most efficient for Gr/Re large and negative (i.e., opposed flow) and that for a fixed value of Gr/Re heat transfer is most efficient when the entry temperature of the fluid is equal to the temperature of the cold wall. Zouhair Ait Hammou [16], studied laminar mixed convection of humid air in a vertical channel with evaporation or condensation at the wall. The results showed that the effect of buoyancy forces on the latent Nusselt number is small. However the axial velocity, the friction factor, the sensible Nusselt number and the Sherwood number are significantly influenced by buoyancy forces.

Barletta [3] studied laminar and fully developed mixed convection in a vertical rectangular duct with one or more isothermal walls. The analysis refers to thermal boundary conditions such that atleast one of the four duct wall is kept isothermal. Huang et al. [9] were studied experimentally the mixed convection flow and heat transfer in a vertical convergent channel. The effect of thermal and mass buoyancy forces on fully developed laminar forced convection in a vertical channel has been studied analytically by Salah El-din [13]. The in-depth literature cited above has revealed that, in spite of the huge amount of knowledge accumulated over the last few decades into the subject of laminar mixed convection in vertical channels, the mixed convection in such geometry is still not fully understood, especially the hydrodynamics of it. For instance, the term “aiding flow” is generally used in the literature as synonym for “up-flow in a heated vertical channel or down-flow for a cooled vertical channel” and vice versa for the term “opposing flow”. The general findings in the literature are that buoyancy effects enhance the pressure drop in buoyancy-aided flow

(upward flow in a vertical heated channel), i.e., there is a monotonic pressure decrease of pressure in the axial direction of upward flow in a vertical heated channel. However, Han [8] proved that in aiding flow situations the pressure build up in the axial direction of the vertical channel. In these two articles it was shown that above certain values of the buoyancy parameter (Gr/Re), the vertical channel can act as a diffuser. However, flow reversal was shown for higher buoyancy effect, which was also pointed out by Han [8] who showed that for more buoyancy effects, the aiding flow is converted to opposed flow. Based on these findings, Han [8] introduced a more precise definition for the terms aiding and opposing flows such that the term aiding flow is used when the external pressure forces and the buoyancy forces works together in the same direction and vice versa for opposing flow.

2 NOMENCLATURE

b	Distance between the parallel plates
C_p	Specific heat of the fluid
Ek	Eckert Number
g	Gravitational body force per unit mass (acceleration)
Gr	Grashoff number, $(g\beta (T_1 - T_0) b^3 / \upsilon^2)$
k	Thermal conductivity of fluid
p	Local pressure at any cross section of the vertical channel
p_0	Hydrostatic pressure
P	Dimensionless pressure inside the channel at any cross section, $(p - p_0) / \rho u_0^2$
Pr	Prandtl Number, $(\mu C_p / k)$
Re	Reynolds number, $((b u_0)/\upsilon)$
T	Dimensional temperature at any point in the channel
T_0	Ambient of fluid inlet temperature
T_w	Isothermal temperatures of circular heated wall
T_1,T_2	Isothermal temperatures of plate 1 and plate 2 of parallel plates
u	Axial velocity component
$\bar{u}$	Average axial velocity
u_0	Uniform entrance axial velocity
U	Dimensionless axial velocity at any point, u / u_0
v	Transverse velocity component

V Dimensionless transverse velocity, v / u_0

x Axial coordinate (measured from the channel entrance)

X Dimensionless axial coordinate in Cartesian, x / (b Re)

y Transverse coordinate of the vertical channel between parallel plates

Y Dimensionless transverse coordinate, y / b

θ Dimensionless temperature

ρ Density of the fluid

ρ_0 Density of the fluid at the channel entrance

μ Dynamic viscosity of the fluid

υ Kinematic viscosity of the fluid, μ/ρ

β Volumetric coefficient of thermal expansion

3 FORMULATION OF THE PROBLEM

We consider the laminar steady flow in a vertical channel. Both channel walls are assumed to be isothermal, one with temperature T_1 and the other with temperature T_2. The system under consideration as well as the choice of the coordinate axes is illustrated in Figure 1.1. The distance between the plates is 'b' i.e., the channel width. The Cartesian coordinate system is chosen such that the x-axis is in the vertical direction that is parallel to the flow direction and the gravitational force 'g' always acting downwards independent of flow direction. The y-axis is orthogonal to the channel walls, and the origin of the axes is such that the positions of the channel walls are y=0 and y=b. The classic boundary approximation is invoked to model the buoyancy effect.

The governing equation for the study viscous flow with the following assumptions are made:

(i) The flow is steady, viscous, incompressible, and developed.

(ii) The flow is assumed to be two-dimensional steady, and the fluid properties are constant except for the variation of density in the buoyancy term of the momentum equation.

After applying the above assumption the boundary layer equations appropriate for this problems are

$$\frac{\partial U}{\partial X}+\frac{\partial V}{\partial Y}=0 \qquad (1)$$

$$U\frac{\partial U}{\partial X}+V\frac{\partial U}{\partial Y}=-\frac{dP}{dX}+\frac{Gr}{\mathrm{Re}}\theta+\frac{\partial^2 U}{\partial Y^2} \quad (2)$$

$$U\frac{\partial \theta}{\partial X}+V\frac{\partial \theta}{\partial Y}=\frac{1}{\mathrm{Pr}}\frac{\partial^2 \theta}{\partial Y^2}+Ek\left(\frac{\partial U}{\partial Y}\right)^2 \quad (3)$$

The form of continuity equation can be written in integral form as

$$\int_0^1 U\,dY=1 \quad (4)$$

The boundary conditions are

Entrance conditions At X = 0, 0≤ Y≤ 1 : U = 1, V = 0, θ = 0, P = 0 (5a)

No slip conditions

At X > 0, Y = 0 : U = 0, V = 0

At X > 0, Y = 1 : U = 0, V = 0 } (5b)

Thermal boundary conditions

At X > 0, Y = 0 : θ = 1

At X > 0, Y = 1 : $\theta = r_T$ } (5c)

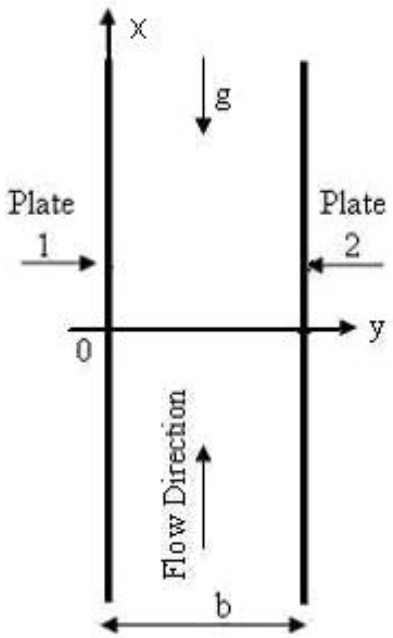

Figure 1: Schematic view of the system and coordinate axes corresponding to Up-flow

In the above non-dimensional parameters have been defined as:

The following non-dimensional variables are used:

$$\left.\begin{aligned} &U = u / u_0,\ V = vb/\upsilon,\ X = x/(b\,Re),\ Y = y/b \\ &P = (p - p_0)/\rho u_0^2,\ Pr = \mu C_p / k,\ Re = (b\,u_0)/\upsilon \\ &Gr = g\beta (T_1 - T_0)\, b^3/\upsilon^2,\ \theta = (T - T_0)/(T_1 - T_0) \end{aligned}\right\} \quad (6)$$

The systems of non-linear equations (1) to (3) are solved by a numerical method based on finite difference approximations. An implicit difference technique is employed whereby the differential equations are transformed into a set of simultaneous linear algebraic equations.

4 NUMERICAL SOLUTION

The solution of the governing equations for developing flow is discussed in this section. Considering the finite difference grid net work of figure 2, equations (2) and (3) are replaced by the following difference equations which were also used in [4].

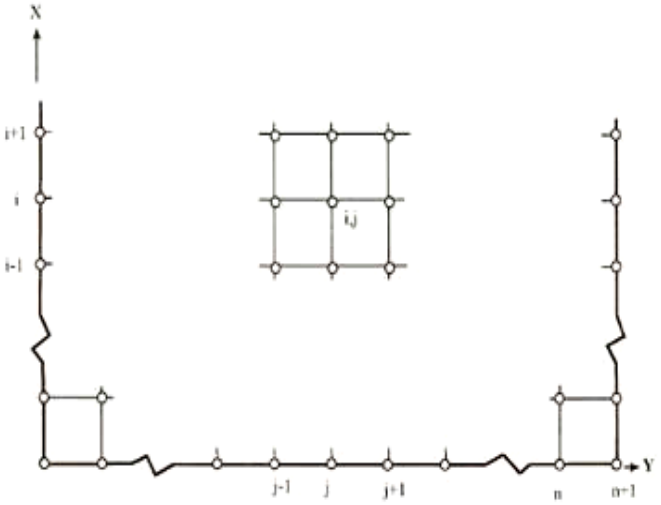

Figure 2: Mesh Network for Difference Representations

$$\begin{aligned} &U(i,j)\frac{U(i+1,j)-U(i,j)}{\Delta X} + V(i,j)\frac{U(i+1,j+1)-U(i+1,j-1)}{2\Delta Y} \\ &= \frac{U(i+1,j+1)-2U(i+1,j)+U(i+1,j-1)}{(\Delta Y)^2} - \frac{P(i+1)-P(i)}{\Delta X} + \frac{Gr}{\mathrm{Re}}\theta(i+1,j) \\ &U(i,j)\frac{\theta(i+1,j)-\theta(i,j)}{\Delta X} + V(i,j)\frac{\theta(i+1,j+1)-\theta(i+1,j-1)}{2\Delta Y} \end{aligned} \quad (7)$$

$$= \frac{1}{\Pr}\frac{\theta(i+1,\, j+1) - 2\theta(i+1,\, j) + \theta(i+1,\, j-1)}{(\Delta Y)^2} + Ek\left(\frac{U(i+1,\, j+1) - U(i+1,\, j-1)}{2\Delta Y}\right)^2 \qquad (8)$$

Numerical representation of the Integral Continuity Equation

The integral continuity equation can be represented by the employing a trapezoidal rule of numerical integration and is as follows:

$$\left[\sum_{j=1}^{n} U(i+1,\, j) + 0.5\left(U(i+1,0) + U(i+1,n+1)\right)\right]\Delta Y = 1$$

However, from the no slip boundary conditions

U(i+1, 0) = U(i+1, n+1) = 0

Therefore, the integral equation reduces to:

$$\left[\sum_{j=1}^{n} U(i+1,\, j)\right]\Delta Y = 1 \qquad (9)$$

A set of finite-difference equations written about each mesh point in a column for the equation (7) as shown:

$$\beta_1 U(i+1,1) + \gamma_1 U(i+1,2) + \xi P(i+1) + \frac{Gr}{\mathrm{Re}}\theta(i+1,1) = \phi_1$$

$$\alpha_2 U(i+1,1) + \beta_2 U(i+1,2) + \gamma_2 U(i+1,3) + \xi P(i+1) + \frac{Gr}{\mathrm{Re}}\theta(i+1,2) = \phi_2$$

- - - -- -- -

- - - -- -- -

$$\alpha_n U(i+1,n-1) + \beta_n U(i+1,n) + \xi P(i+1) + \frac{Gr}{\mathrm{Re}}\theta(i+1,n) = \phi_n$$

where

$$\alpha_k = \frac{1}{(\Delta Y)^2} + \frac{V(i,j)}{2\Delta Y}, \quad \beta_k = -\left[\frac{2}{(\Delta Y)^2} + \frac{U(i,j)}{\Delta X}\right] \quad \gamma_k = \frac{1}{(\Delta Y)^2} - \frac{V(i,j)}{2\Delta Y},$$

$$\xi = \frac{-1}{\Delta X}, \quad \phi_k = -\left[\frac{P(i) + U^2(i,j)}{\Delta X}\right]$$

for k = 1,2… n

A set of finite-difference equations written about each mesh point in a column for the equation (8) as shown:

$$\overline{\beta}_1\theta(i+1,1) + \overline{\gamma}_1\theta(i+1,2) + \text{----------} = \overline{\phi}_1 - \overline{\alpha}_1,$$

$$\bar{\alpha}_2\theta(i+1,1)+\bar{\beta}_2\theta(i+1,2)+\bar{\gamma}_2\theta(i+1,3)+\text{----------}=\bar{\phi}_2$$

$$\bar{\alpha}_n\theta(i+1,n-1)+\bar{\beta}_n\theta(i+1,n)=\bar{\phi}_n-r_T\bar{\gamma}_n$$

where

$$\bar{\alpha}_k=\frac{1}{\Pr(\Delta Y)^2}+\frac{V(i,j)}{2\Delta Y},\qquad \bar{\beta}_k=-\left[\frac{2}{\Pr(\Delta Y)^2}+\frac{U(i,j)}{\Delta X}\right],\qquad \bar{\gamma}_k=\frac{1}{\Pr(\Delta Y)^2}-\frac{V(i,j)}{2\Delta Y},$$

$$\bar{\phi}_k=-\frac{U(i,j)\theta(i,j)}{\Delta X}-Ek\left(\frac{U(i+1,j+1)-U(i+1,j-1)}{2\Delta Y}\right)^2$$

for k = 1,2… n

Equation (12) can be written as

$$V(i+1,j)=V(i+1,j-1)-\frac{\Delta Y}{2\Delta x}(U(i+1,j)+U(i+1,j-1)-U(i,j)-U(i,j-1)),\ j=1,2,.....n \qquad (10)$$

The numerical solution of the equations is obtained by first selecting the parameter that are involved such as Gr/Re, M, Pr and r_T. Then by means of a marching procedure the variables U, V, θ and P for each row beginning at row (i+1)=2 are obtained using the values at the previous row 'i'. Thus, by applying equations (7), (8) and (9) to the points 1, 2, ..., n on row i, 2n+1 algebraic equations with the 2n+1 unknowns U(i+1,1), U(i+1,2), ..., U(i+1,n), P(i+1), θ(i+1,1), θ(i+1,2), . ., θ(i+1, n) are obtained. This system of equations is then solved by Gauss – Jordan elimination method. Equations (10) are then used to calculate V(i+1,1), V(i+1,2), ..., V(i+1,n).

5 RESULTS AND DISCUSSION

The numerical solution of the equation is obtained first selecting the parameters that are involved such as Gr/Re, r_T, Ek and Pr. For fixed Pr = 0.7 and different values of Gr/Re, Ek and r_T, the velocity profiles are shown in figures 3 to 11, the temperature profiles are shown in figures 12 to 16 and the pressure profiles are shown in figures 17 and 18.

Figures 3 to 5 executive velocity profiles for fixed X and r_T, as can be seen, vary closed to the channel inlet, the heating effects are not yet and further down stain, the heating causes the fluid accelerate near the hot wall and decelerate near the heated wall resulting distortion of velocity profiles to satisfy the continuity principle. However the velocity profiles recovers and attains it asymptotic fully developed parabolic profile. A skewness in the velocity

profiles also appear as the fluid moves towards the hot wall (Y=1). The smaller r_T, the greater is the skewness. On the other hand increased buoyancy introduces a more severe distortion as illustrated in figures 6 to 11. It is clear that the flow reversal will take place for asymmetrical heated channels with high values of the buoyancy parameter Gr/Re. Values of the buoyancy parameter Gr/Re that represents heating rates that are enough to create severe flow reversal at the cooler wall in asymmetrically heated channels usually results in a flow instability and consequentially numerical instability. The velocity profiles are not effect for increasing Eckert number Ek and for fixed Prandtl number Pr and buoyancy parameter Gr/Re.

The development of the temperature field is exemplified by figures 12 to 16. The effect of the buoyancy parameter Gr/Re is felt in the developing regions, where the buoyancy decreases the temperature in the region adjacent to the hot wall. While increasing the temperature else where in the flow. Thus the buoyancy tenses to equalize the temperature in the fluid. It is seen that the temperature profiles are effect for increasing Eckert number Ek and for fixed Gr/Re and Prandtl number Pr at r_T for different fixed X values. This type of temperature profiles is consistent with this pertinent developing velocity profiles that have two peaks near the two heated walls and minimum velocities near the core of the channel, where that heat did not penetrate yet. These profiles show clearly how is heat takes time until it penetrates the fluid layers reaching the core at large enough distances from the channel entrance till it reaches fully developed region where all the fluid layers will attain the same temperature of a dimensionless value of 1.

Figures 17 and 18 shows the variation of the dimensionless pressure parameter P for r_T=0.5 and r_T = 1. The figures indicate the steam wise variation of the parameter at different buoyancy parameter Gr/Re for fixed. In the upper range of Gr/Re the maximum pressure occurs at about the point where buoyancy effects begin to be felt. In the same range it is also observed that P becomes positive when the center line velocity attains a value of less than that of the entry velocity. The pressure profiles are not effect for increasing Eckert number Ek and for fixed Prandtl number Pr and buoyancy parameter Gr/Re.

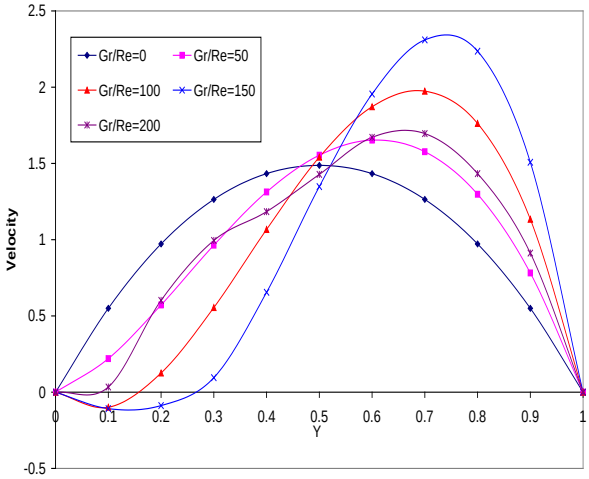

Figure 3: Velocity profile for fixed $r_T = 0$ and X = 0.04

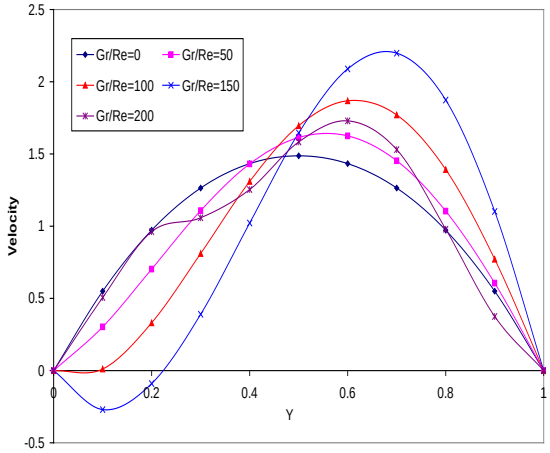

Figure 4: Velocity profile for fixed $r_T = 0.5$ and X = 0.04

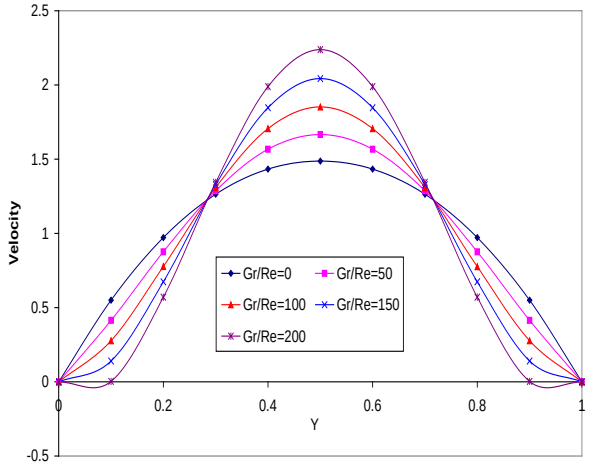

Figure 5: Velocity profile for fixed $r_T = 1$ and X = 0.04

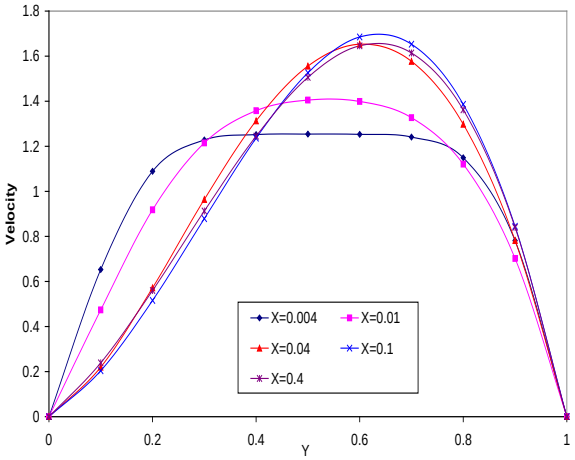

Figure 6: Velocity profile for fixed $r_T = 0$ and Gr/Re = 50

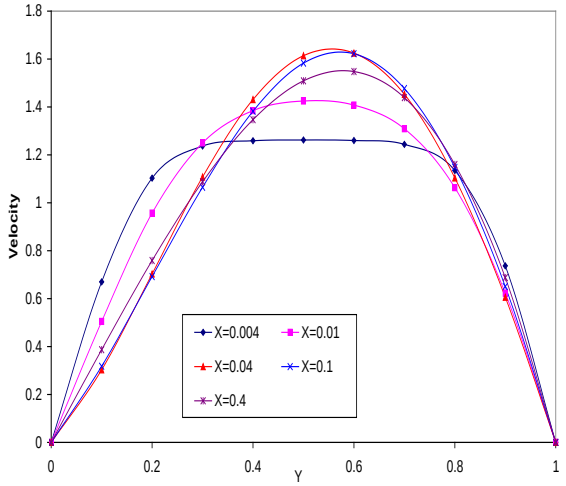

Figure 7: Velocity profile for fixed $r_T = 0.5$ and Gr/Re = 50

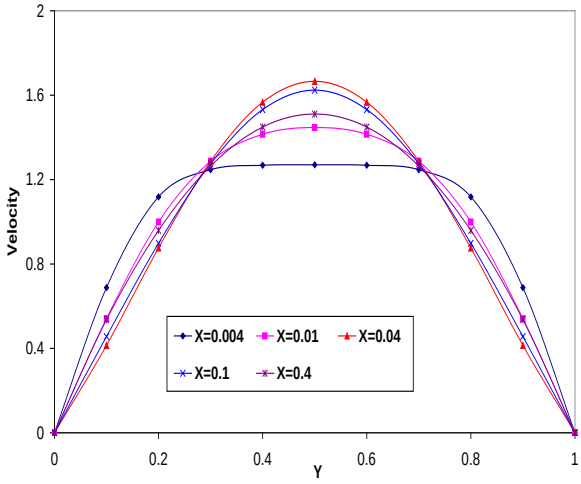

Figure 8: Velocity profile for fixed $r_T = 1$ and Gr/Re = 50

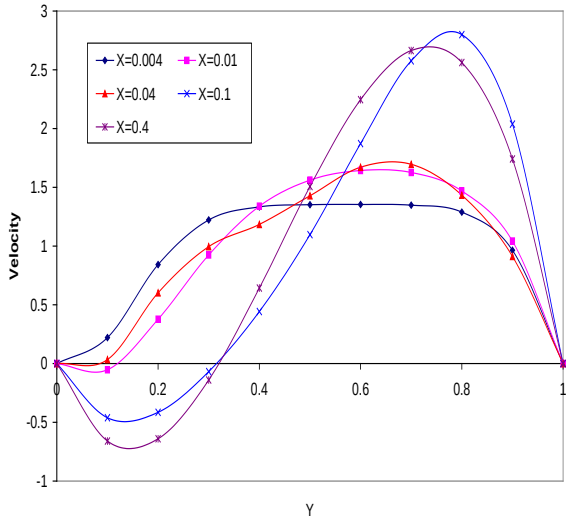

Figure 9: Velocity profile for fixed $r_T = 0$ and Gr/Re = 200

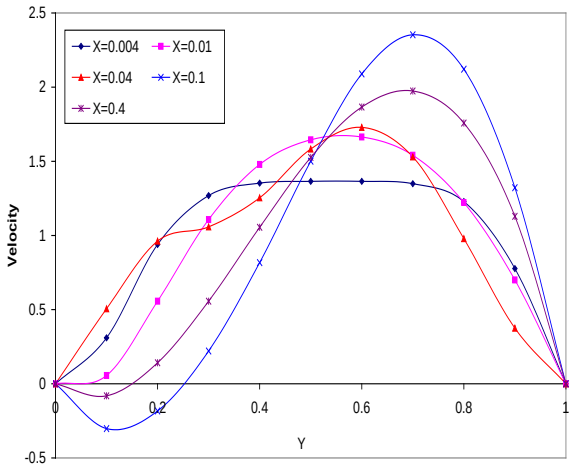

Figure 10: Velocity profile for fixed $r_T = 0.5$ and Gr/Re = 200

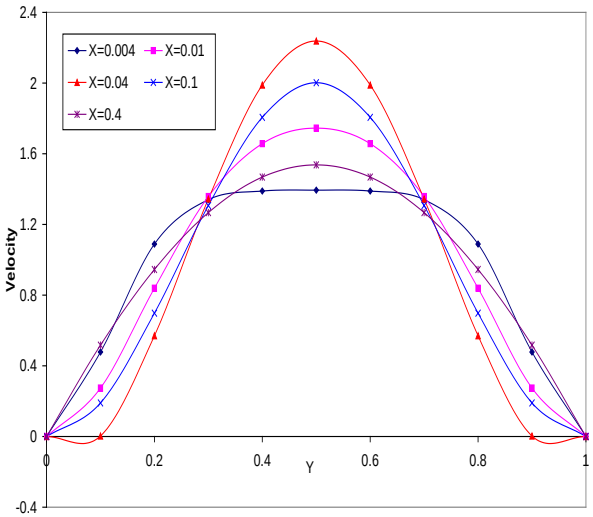

Figure 11: Velocity profile for fixed $r_T = 1$ and Gr/Re = 200

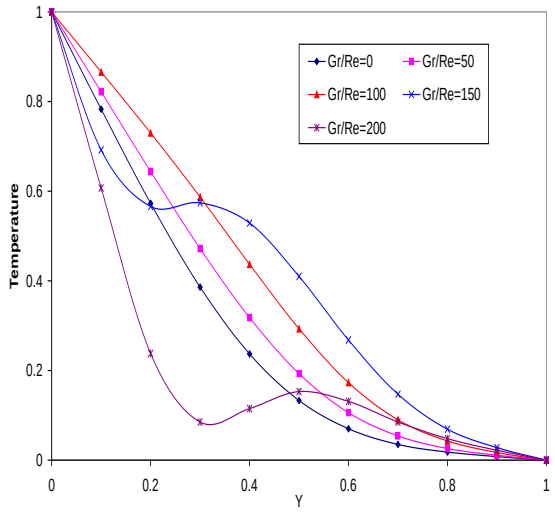

Figure 12(a): Temperature profile for fixed $r_T = 0$, Ek = 0 and X = 0.04

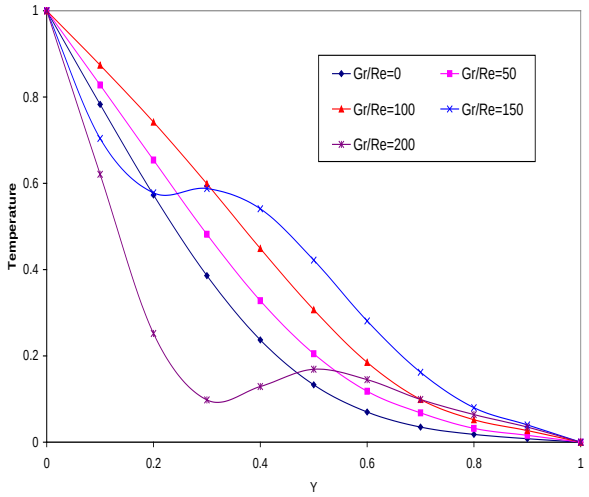

Figure 12(b): Temperature profile for fixed $r_T = 0$, Ek = 5 and X = 0.04

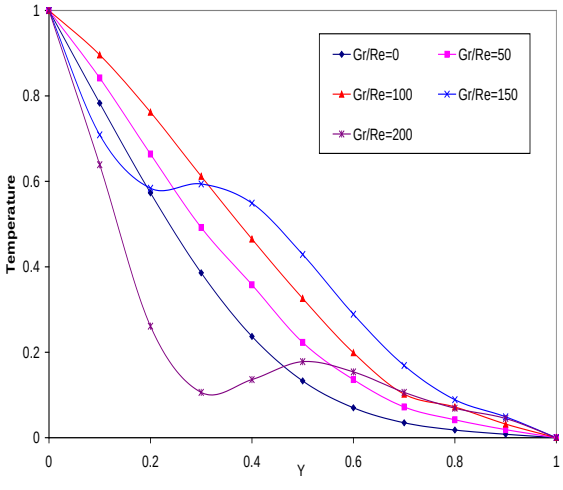

Figure 12(c): Temperature profile for fixed $r_T = 0$, Ek = 10 and X = 0.04

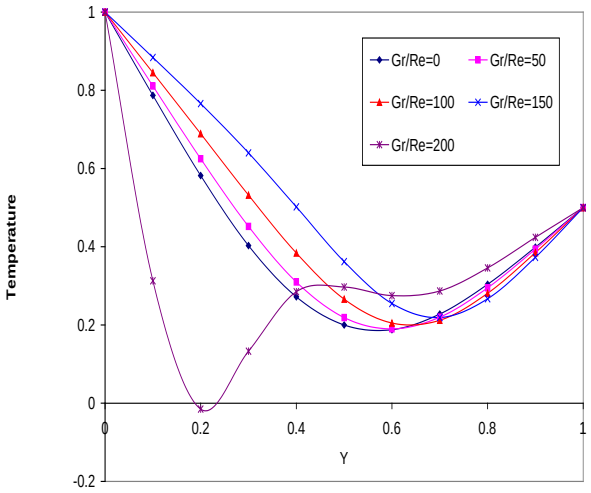

Figure 13(a): Temperature profile for fixed $r_T = 0.5$, Ek = 0 and X = 0.04

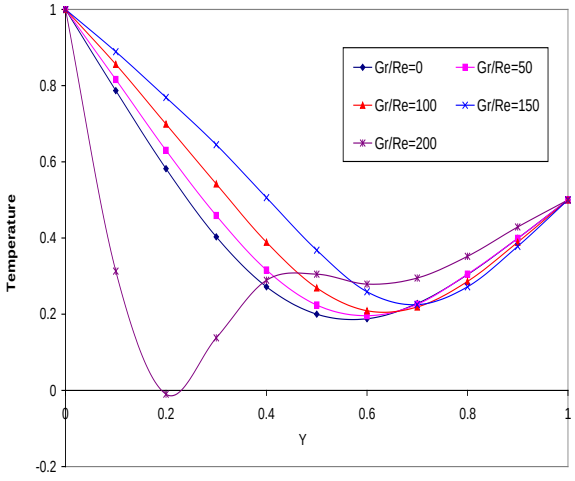

Figure 13(b): Temperature profile for fixed r_T=0.5, Ek = 5 and X = 0.04

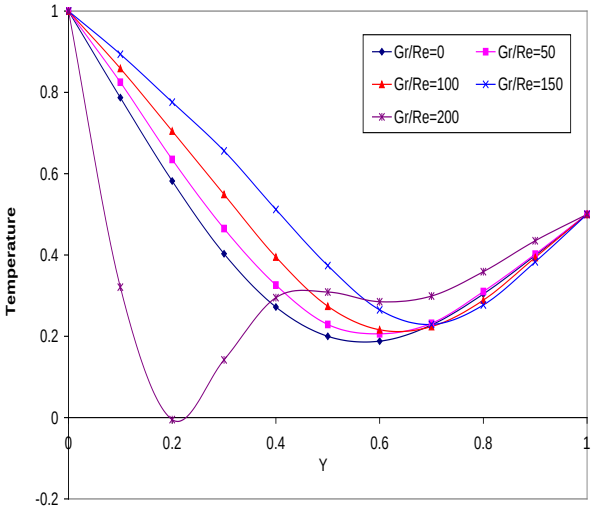

Figure 13(c): Temperature profile for fixed $r_T = 0.5$, Ek = 10 and X = 0.04

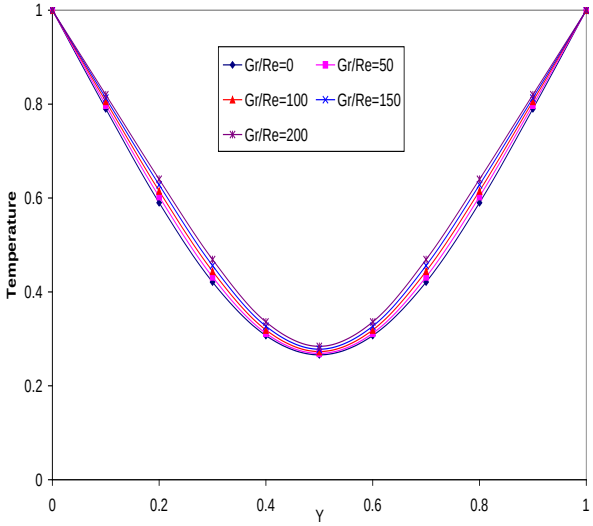

Figure 14(a): Temperature profile for fixed $r_T = 1$, Ek = 0 and X = 0.04

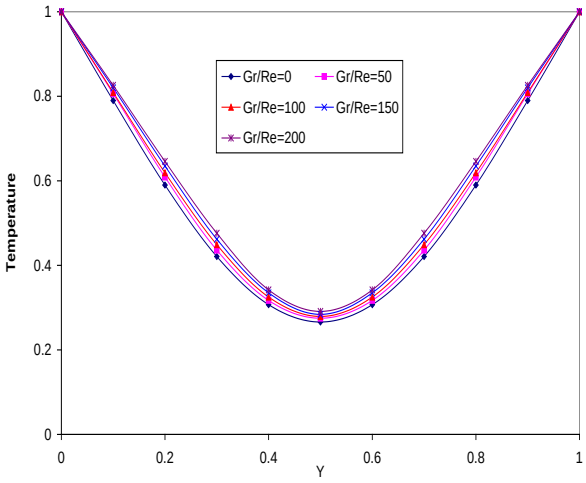

Figure 14(b): Temperature profile for fixed $r_T = 1$, Ek = 5 and X = 0.04

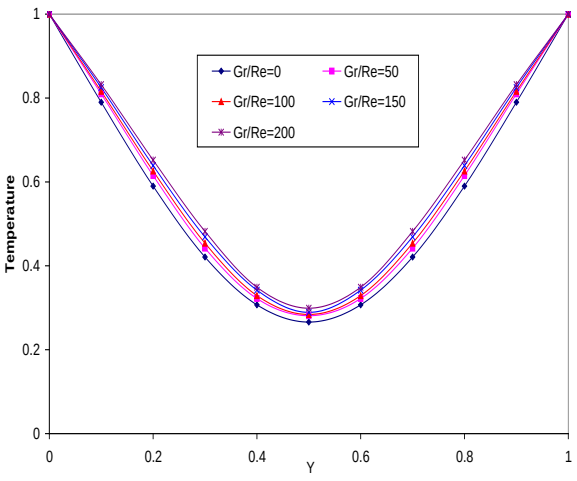

Figure 14(c): Temperature profile for fixed $r_T = 1$, Ek = 10 and X = 0.04

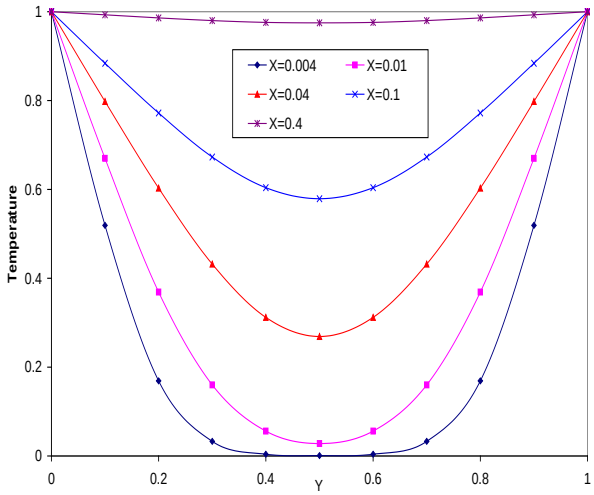

Figure 15(a): Temperature profile for fixed $r_T = 1$, Ek = 0 and Gr/Re = 50

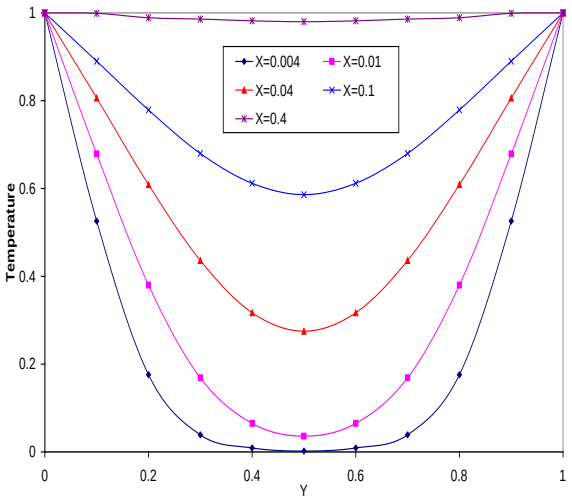

Figure 15(b): Temperature profile for fixed $r_T = 1$, Ek = 5 and Gr/Re = 50

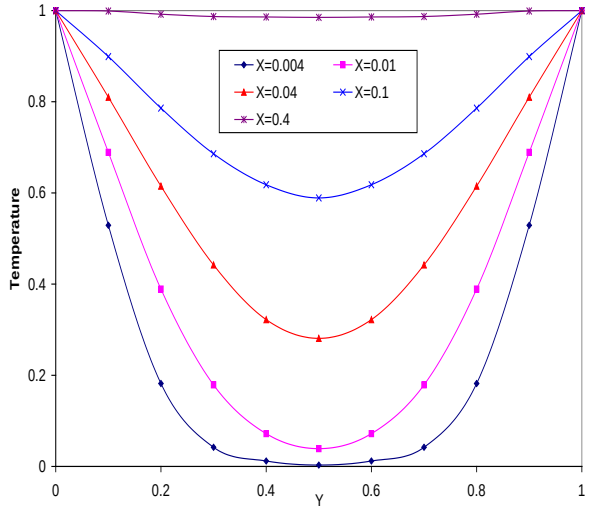

Figure 15(c): Temperature profile for fixed $r_T = 1$, Ek = 10 and Gr/Re = 50

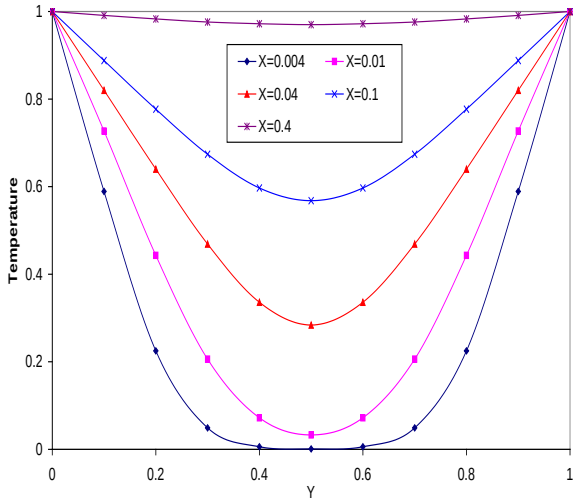

Figure 16(a): Temperature profile for fixed $r_T = 1$, Ek = 0 and Gr/Re = 200

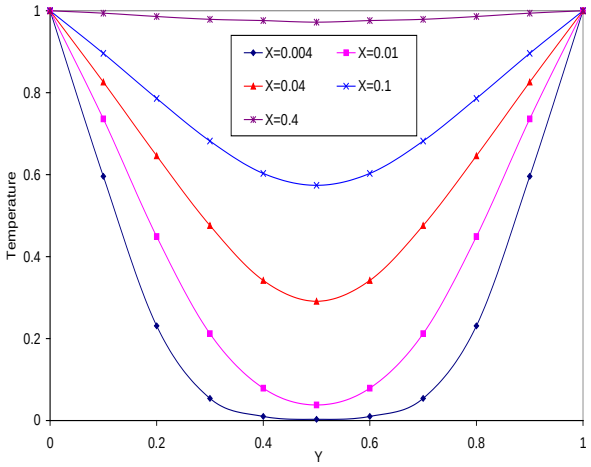

Figure 16(b): Temperature profile for fixed $r_T = 1$, Ek = 5 and Gr/Re = 200

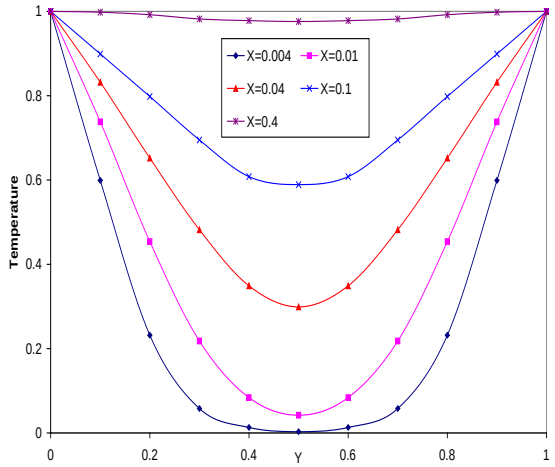

Figure 16(c): Temperature profile for fixed $r_T = 1$, Ek = 10 and Gr/Re = 200

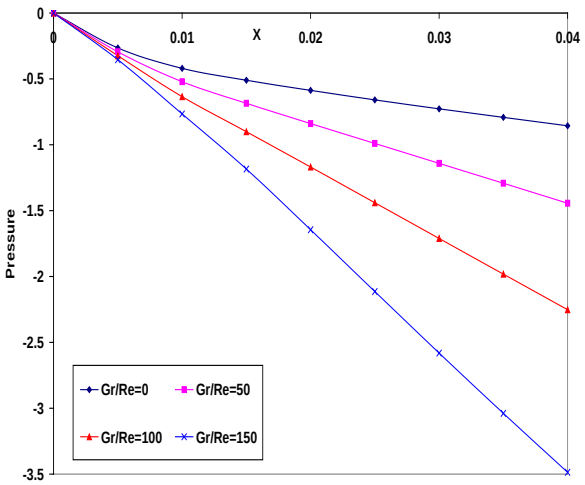

Figure 17: Pressure profile for fixed $r_T = 0.5$

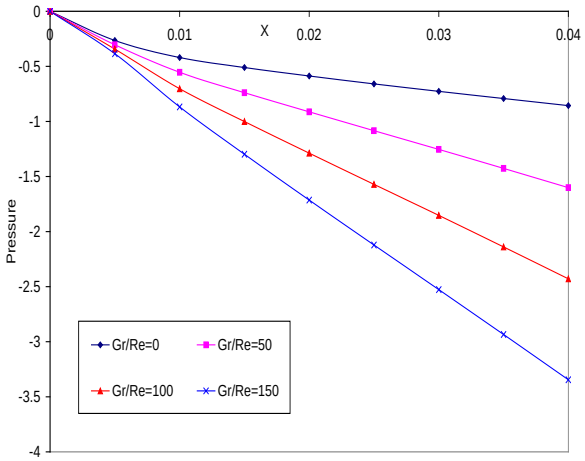

Figure 18: Pressure profile for fixed $r_T = 1$

REFERENCES

1. Aung. W., and Worku, G., ASME. J. Heat Transfer, Vol. 108, pp.299- 304, 1986.
2. Aung. W., and Worku, G., ASME. J. Heat Transfer, Vol. 108, pp.485- 488, 1986.
3. Barletta, A., Int. J. Heat Mass Transfer, Vol.44, pp.3481-3497, 2001.
4. Bodoia, J.R., and Osterle, J.F., ASME. J. Heat Transfer, Vol. 84, pp.40-44, 1962.
5. Boulama, K., and Galanis, N., ASME J. Heat transfer, Vol.126, pp.381-388, 2004.
6. Cebeci, T., Khattab, A.A., and Lamont, R., 7th Int. Heat Transfer Conf., Vol.2, pp.419-424, 1982.
7. Hamadah, T.T. and Wirtz, R.A., ASME J. Heat transfer, Vol.113, pp.507-510, 1991.
8. Han, J.C., ASME. J. of Fluid Engineering, Vol. 115, pp.41-47, 1993.
9. Huang, T.M., Gau, C., and Aung, Win., Int. J. Heat Mass Transfer, Vol.38, No.13, pp.2445-2456, 1995.
10. Inagaki, T., and Komori, K., Numerical Heat Transfer, Part-A, 27(4), pp.417-431, 1995.
11. Ingham, D.B., Keen, D.J. and Heggs, P.J., ASME. J. Heat Transfer, Vol. 110, pp.910-917, 1988.
12. Reddy B.R.B., Int. J. of Mathematics Research, Vol.3, No.6, pp.531-556, 2011.
13. Salah El-Din, M.M., Int. Comm. Heat Mass Transfer, Vol.19, pp.239-248, 1992.
14. Writz, R.A., and Mckinley, P., ASME Publication, HTD, Vol.42, pp.105-112, 1985.
15. Yao. L.S., Int. J. Heat Mass Transfer, Vol.26(1), pp.65-72, 1983.
16. Zouhair Ait Hammou, Brahim Benhamou, Galanis, N., and Jamel Orfi., Int. J. of Thermal Sciences, Vol. 43, pp.531-539, 2004.